Metal Organic Chemical Vapor Deposition of Oxide Films for Advanced Applications

G. S. Tompa, L.G. Provost, and J. Cuchiaro
Structured Materials Industries, Inc., 120 Centennial Ave., Piscataway, NJ 08854
www.structuredmaterials.com

Transparent and conductive films, well known for their historical roles in solar cells and displays, are receiving renewed attention due to the need for increased performance requirements and for advanced applications that are being developed. While there are many methods to deposit thin films, Metal Organic Chemical Vapor Deposition (MOCVD) is of particular importance for producing high quality films over large areas in a manufacturing mode. Important features of MOCVD include excellent conformality of deposited films, elimination of pinhole type defects, the absence of radiation process induced damage, and low particle counts. Over the past several years, we have devoted our efforts to developing and advancing the MOCVD process and systems technology, primarily using Rotating Disk Reactors (RDRs), and advancing the breadth of deposited oxide materials for several applications. The deposition technology, which will be reviewed, has been scaled from a 5" deposition diameter through to 12" diameter. We have found that MOCVD has been able to produce a wide range of oxide materials under a variety of processing conditions and that the technology is readily scalable. Systems technology, processing parameters and results for MOCVD of transparent (visible and IR) and conductive oxides will be reviewed. Advanced materials development and applications such as producion of luminescent or p-type ZnO and related oxides, development of amorphous, polycrystalline and single crystal films and applicability in photovoltaics, LEDs or lasers, detectors, and others will also be addressed.

INTRODUCTION

Transparent conductive oxides, or TCOs, are commonly present in displays, electrochromic windows, and photovoltaics, and may soon find major roles in optoelectronic devices. A more detailed listing of applications would include: displays, low emissivity windows (temperature control) and other light regulating devices (such as self-driving mirrors), transparent heaters (mirrors, windows), esthetic coatings, photovoltaics, touch sensitive controls, electromagnetic shielding (as found on microwave ovens and stealth fighters), static dissipaters, and so on. The desire for higher conductivity, p-type conductivity and TCOs with application-tailored properties is immense and growing. We herein review the approach we have developed to investigate and produce advanced TCO and related film, and then focus on reviewing TCO results in one base material system. An excellent overview of TCOs is presented in the August 2000 issue of the MRS Bulletin as a general starting point for reviewing TCO technology.

FOCUS ON ZINC OXIDE TCO

A natural outgrowth of display technology efforts is the development of advanced transparent and conductive oxides (TCO). ZnO is one such promising TCO. Early (prior to ~1980) and continuing studies of ZnO focused on transducers in surface acoustic wave (SAW) devices because ZnO has one of the largest electromechanical coupling coefficients of all non-ferroelectric materials. The majority of studies emphasized surface morphology and preferred orientation effects, rather than the electrical and optical properties of ZnO films[1]. ZnO ceramics with minor additives such as Bi_2O_3, SB_2O_3, CoO, MnO,

and Cr_2O_3 show very nonohmic I-V characteristics[2] and are used extensively as varistors in protecting power and signal level electrical circuits against dangerous voltage surges[3]. Further, ZnO is a transparent conductive oxide, which can be "alloyed" with a variety of materials to change its properties for product benefit. These properties allow the exciting possibility of being able to arbitrarily form transparent conducting and non-conducting zones for advanced device designs. While we have investigated a great many oxide materials, in this work we will focus primarily on ZnO based materials.

Several deposition techniques have been applied to grow ZnO films: evaporation[4,5], r.f.[6,7,8,9], d.c.[10,11,12,13] magnetron sputtering, ion beam sputtering [14], spray pyrolysis[15,16,17], sol-gel process[18], pulse-laser deposition[19], chemical beam deposition[20], and metal-organic chemical vapor deposition (MOCVD)[21,22,23,24,25,26,27,28,29,30,31,32]. Highly conductive n-type and transparent ZnO films were readily obtained by doping with B, Al, Ga, In, and F. Al is the most commonly studied dopant in ZnO films in all growth techniques. Igascki et al.[6] reported growth of ZnO:Al with a resistivity as low as 1.4×10^{-4} Ωcm from r.f. sputtering. Sato et al.[10] reported a resistivity of 6×10^{-4} Ωcm from d.c. sputtering. Using chemical beam deposition technique, the same group reported a resistivity of 3.4×10^{-4} Ωcm[33]. Tang & Cameron[34] obtained a resistivity of 7×10^{-4} Ωcm from sol-gel process. Hu and Gorden[35] achieved a resistivity of 3.0×10^{-4} Ωcm from MOCVD process. These data have shown that doped ZnO has equivalent electrical characteristics as ITO films from a variety of deposition techniques.

FOCUS ON MOCVD

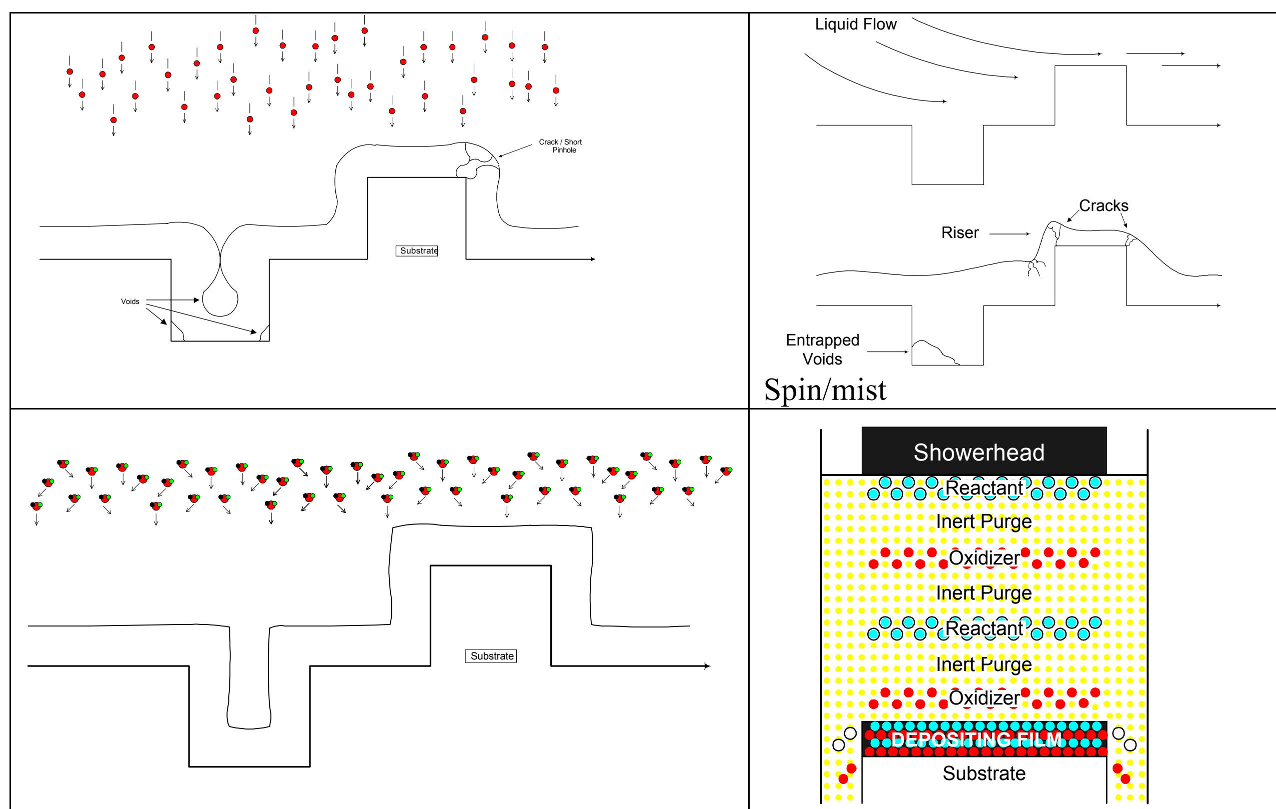

Figure 1. Comparison of major deposition technologies: (a) Physical Vapor Deposition, (b)spin/mist deposition, (c) chemical vapor deposition, and (d) schematic representation of alternating layer chemical vapor deposition in an RDR.

Figure 1 contrasts the primary methods for depositing high quality films. The methods are physical vapor deposition (PVD), spin/mist deposition, (CVD), and alternating layer (AL) CVD. PVD is a line of sight technology and is used very successfully when grading, complex multiplayer doped/mixed

alloy structures, or crystalline films are not needed. The spin/mist approach is also useful for blanket coverages, but may suffer from voids or defects in thermal processing. CVD (and its refined form AL-CVD) offer tremendous advantages to other techniques in terms of conformality, grading, achievement of complex thin and multilayer structures, including epitaxial films, and its ability to adapt to deliver many complex and graded composition films. Our efforts, as described below, focus on using RDR-MOCVD to produce a variety of oxide films.

Table I. RDR-MOCVD Tool Demonstrated Material Capabilities and General Application Areas

Type	Example Materials	Applications
Oxides:	ZnO:Ga/Al/B/F/In, ZnO:Zn, ZnO:N, Zn_2GeO_4:Mn, $ZnIn_2O_4$:Mn/Ga, Zn_2SiO_4:Mn, $ZnGa_2O_4$:Mn/Ga, Al_2O_3, SiO_2, CuAgO/CuAlO/Cu, CuGaO, BST, PZT & SBT, YBa_2Cu_3O, CeO, InO, TCOs, Ta_2O_5, ZrO, MnO, HfO, CeO, MnO, MgO	Displays (TCOs, heaters, Phosphors…) Memory (DRAM, NVRAM, PRAM…) Varistors SAW/microwave
Silicon/:	Si, SiGe, SiGeC, ….	Opto-electronics/
Carbides:	SiC, Diamond, ….	Waveguides
Nitrides:	InGaAlN, Si_3N_4, TiN, BN, ….	Dielectrics
III-Vs:	GaAs, InP, InSb, InGaAsSb, AlGaAs, …. Protective coatings	Pyroelectrics Compound semiconductors
II-VIs:	HgCdTe, CdTe, ZnTe, ZnSe, ….	
Metals:	Cu, W, Al, Pt, Ru, Ir, ….	

EXPERIMENTAL

At SMI, we have developed Low Pressure (and Plasma Enhanced) Metal Organic Chemical Vapor Deposition (LP-MOCVD) systems to produce an array of oxides as listed in Table I[36,37,38]. The system employs a vertical high speed Rotation Disk Reactor (RDR), as shown in Figure 2, with radially distributed multi-gas-injectors on its top flange (for uniformity over large areas) and a separate oxygen injector directly above the sample platter (minimizing pre-reactions). The high speed rotating disk can be rotated through 1000 RPM. The high speed rotation and high gas velocity induces laminar, non-recirculating forced convection flow in the system. Samples are heated by a fixed radiative heater below the rotating susceptor. Thermophoresis drives particles from the deposition surface. The temperature, pressure, rotation, and mass-flow rates are monitored and controlled by a computer. A carrier gas is used to carry reactants, in vapor form, from bubbler, sublimator, or flash evaporation sources. Reactant sources and delivery lines can be temperature controlled. The carrier gas is further diluted and enters the reactor through the reactor top flange multi-inlet-injector manifold. The radially distributed injection manifold in the RDR is used to achieve radial composition grading in order to optimize thickness and composition across the deposited films. An oxidizer injector is also used for plasma enhanced mode operation in an upstream plasma column configuration for plasma enhanced CVD, as we have done with N_2, N_2O_2, and NH_2 in doping ZnO p-type. Other gases can also be introduced through this port for process enhancement. Further, the system geometry is ideal for alternating layer CVD (ALCVD), as we have demonstrated in the past. Typical process parameters are reviewed in Table II.

A significant a-priori tool in reactor design and process development is modeling. To perform modeling, we use CFD-ACE+ in conjunction with university researchers to develop and improve upon our reactor designs and process parameters. Figure 2(a) depicts the results of one such reactor modeling shown schematically in Figure 2(b) and photographically in 2(c).

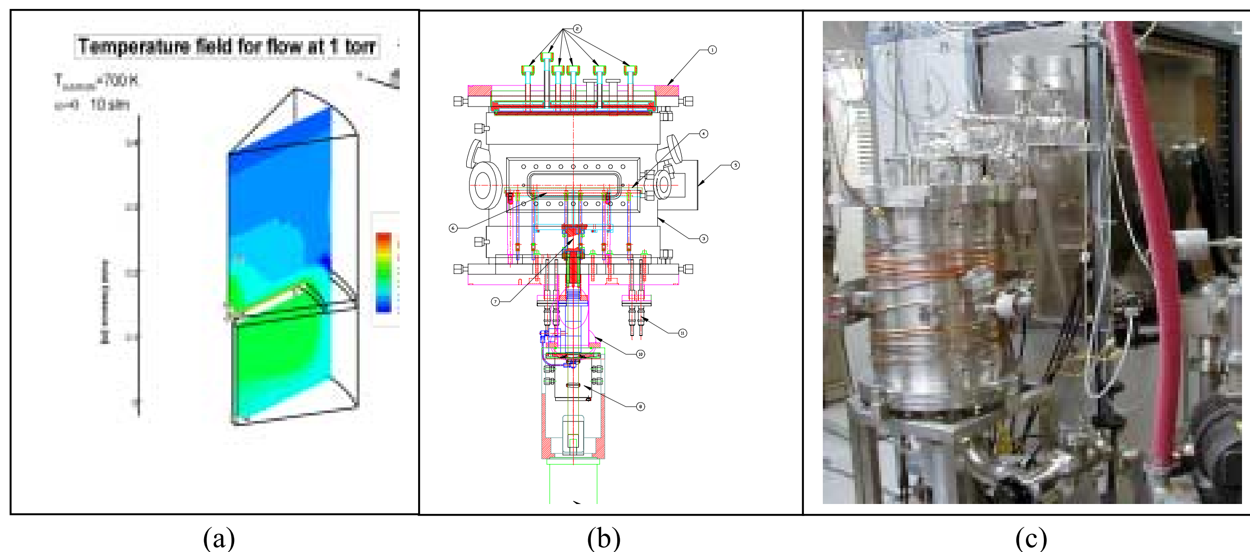

(a) (b) (c)

Figure 2. (a) Example graphic result of process modeling used to guide design and process development; (b) cross-section of a latest generation RDR, and (c) photograph of an actual reactor capable of processing up to 300 mm wafers.

Figure 3 depicts a generalized schematic of one of the RDR LP-MOCVD systems used in these studies. The RDR systems have great flexibility in producing a wide range of materials, from doped and homogeneous to full alloy materials. Several different vapor sources can be simultaneously introduced into our RDR systems. Importantly, in addition to demonstrating results with Zn, Si, Ga, Al, Mn, Ba, Sr, Tr, Pb, Bi, Ta, Ge, In, B, Ce, Mn, Cu, Ag, and Mg, this system is also well capable of transporting a variety of other reactants, including sublimed, bubbled, flash evaporated, or gas sources for film formation.

Table II. General RDR-MOCVD Process Parameters

Reactor Details

Type: Vertical Rotating Disk, low pressure, hot walled
Chamber Pressure: Typically 10-40 Torr
Base Pressure: 5 mTorr

Rotating Disk Reactor Parameters

Disk-Wall Flow	Disk/Reactor Diameter ~70% (~equal areas)
Disk Gas Pumping	$\propto (WP)^{.5}$
Vertical boundary Layer	$\propto (1/WP)^{.5}$
Reynolds Number	$r^2 d\, w/\nu_\infty$ (~200-3000)
Mixed Convection Parameter	$g(T_d/T_\infty - 1)W(WV_\infty)^{.5}$ (<2)
Typical SMI	
254 mm height	300 mm platter
400 mm wall	250/700°C
Re 275	0.13 MCP

General Process Parameters

Zinc partial pressure range: 0.005-0.009 Torr

O_2:Zn ratio range:	1 - 150
Total flow of gases:	10-15 slm
Deposition time:	10-40 minutes
Rotational speed:	10-1000 rpm (600-900 typ.)
Substrate temperature:	375-650ºC

Precursor Materials

Zinc source: di-ethyl zinc (DEZ), source temperature 35ºC, pressure range 400-425 Torr
Gallium source: tri-ethyl gallium (TEGa), source temperature 27ºC, pressure 400 Torr
Carrier and Push gas: N_2 or Ar Oxidizer: Oxygen
Single Glass Sheet dimensions: 14.4 cm x 9.4 cm

The main features of a MOCVD system, as shown in Figure 3, are: (i) the gas and vapor delivery sub-system, (ii) the deposition reactor assembly, and (iii) the exhaust sub-system. Not shown in the schematic are substrate handling and the process control systems. The gas and vapor delivery system is used to provide the precursors to the materials to be deposited into the reactor. The precursors must be

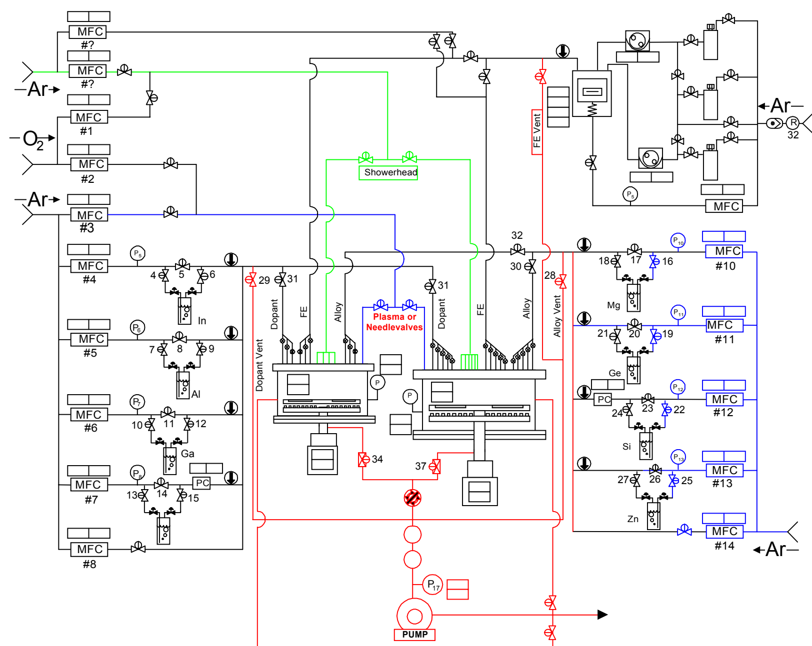

Figure 3. Oxide RDR-MOCVD dual reactor schematic; one of the systems used in the work presented here.

Attributes of a RDR-MOCVD system.

- Flexible processing proven for oxides, metals, and compound semiconductors
- Designed flow dynamics and thermal profiles
- Separate and distributed reactant injection within uniform showerhead flow
- Compatible with nano-scale structures
- High speed rotation enhanced efficiency
- Particulate minimizing through thermophoresis
- Scalable and modular
- Economical
- MESC compatible
- Reliable and safe
- Process parameters computer controlled
- In-situ monitoring compatible
- Plasma enhanced/etching compatible

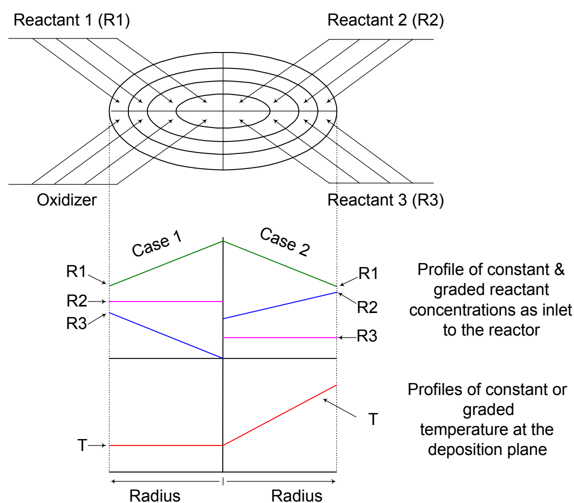

Figure 4. Depiction of unique ability of RDR geometry to adapt to combinatorial synthesis applications by radial grading of either or both of the temperature and precursor concentration gradients.

delivered cleanly and in proper amounts and distributions across the substrate. The reactor must present a precisely controlled environment conducive to efficient deposition of films onto the substrate alone. The exhaust system must efficiently and safely remove effluent from the system. A substrate transfer system is implicitly efficient to system operation because automation of the transfer process eliminates chance handling hazards and system contamination exposures. It also acts as a buffer to the process chamber when hazardous gases are used. Finally, and most important, a process control system is required to guarantee process repeatability, real time feedback and correction and documentation of complete process parameters. Process control systems also offer a full line of self-diagnostics and interface routes.

The general RDR geometric configuration is unique in the CVD world, lending itself to combinatorial synthesis (CS) studies. Figure 4 depicts how the reactor may be utilized to produce compounds in a CS mode. First, because of the rotation and radial symmetry, an array of precursors may be introduced through different area injection

zones with different radial concentrations. Second, through the use of concentric filaments, a thermal radial gradient may also be generated. Either or both gradients together are sufficient to produce films of widely varying composition and/or structural properties.

Figure 5 depicts some of the unique features achievable with CVD process technology. First, Figure 5(a) shows placement of a flash evaporator, which can be used to evaporate low volatility compounds such as those used for Sr, Y, Ca, La, Zr, Bi, and so on. Figure 5(b) and (c) show placement and utilization, respectively, of plasma enhancement to the process. Plasma enhancement imparts effective temperatures exceeding thousands of degrees to stimulate reactions that would otherwise not be possible with conventional heating methodologies.

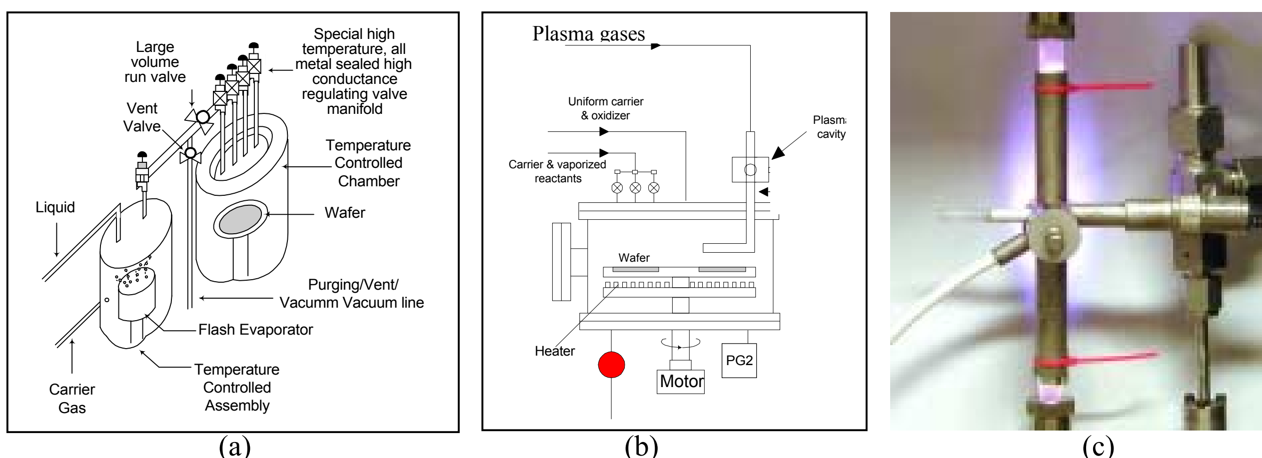

Figure 5. (a) Cross-sectional schematic of RDR with close spaced Flash Evaporator used to produce vapors of low volatility compounds, (b) test reactor schematic showing internal placement of a plasma column, and (c) photograph of upstream plasma column with nitrogen plasma ignited.

RESULTS

SMI began earnest development of ZnO based conductive oxides in 1997, with the award of BMDO/ONR Contract No:N00014-97-C0064. We herein briefly summarize results stemming from this and several subsequent development efforts. Using process parameters consistent with Table II, we deposited an array of highly transparent and conductive films. For high conductivity, we typically doped the films with Ga or Al. The obtained ZnO:Ga film morphologies are smooth and specular. Fig. 6(a) is a typical SEM photo image of a 800 nm thick ZnO/glass film at a magnification of ×30000. The sharp cleavage edge indicates that the films are highly adherent to the substrate. A polycrystalline grain size of

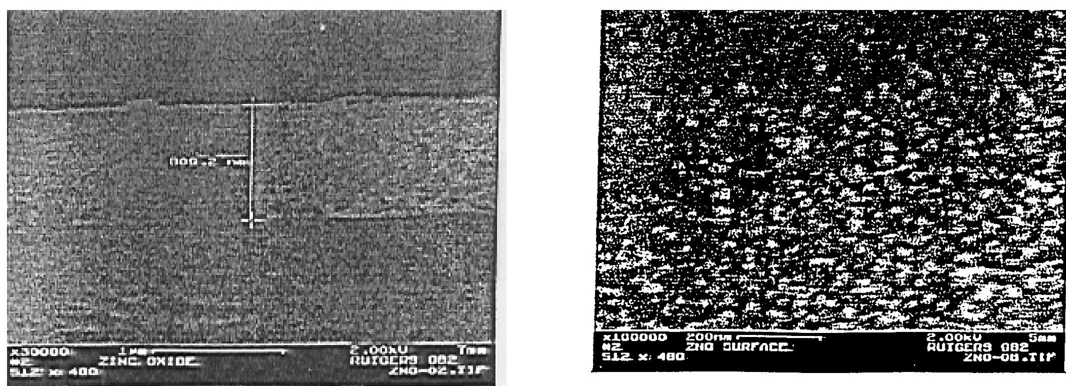

Figure 6. (a) SEM cross-section and (b) surface images of a ZnO film grown on a glass substrate at 400 °C.

about 40 nm was observed under a magnification of ×100000 as shown in Fig. 6(b). Pre-reaction between O_2 and DEZn was not noticeable until the growth temperature was raised above ~500 °C. Fig. 7 depicts the sheet resistance as a function of Ga concentration incorporated in the ZnO film. The Ga concentrations were measured with SIMS and the sheet resistances were measured with standard 4-point probe. Quantification of the gallium concentration in the ZnO:Ga film was accomplished by analyzing Ga-doped and undoped ZnO films by SIMS, correlated with ion implanted standards of Ga in SiO_2 because ZnO standards are unavailable. Doping with Al showed a similar behavior.

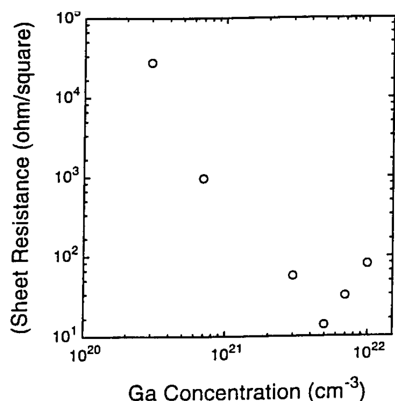

Figure 7. Sheet resistance as a function of Ga concentration (as determined by SIMS and 4-point probe).

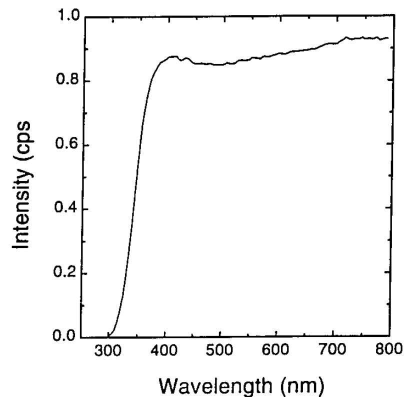

Figure 8. A typical transmittance spectra of an as-grown ZnO:Ga film on a Corning 7059 glass substrate grown at 400°C with Ga concentration of 1 x 10^{21} cm^{-3}.

The transmittance measurements were made for the Ga doped ZnO films on Corning 7059 glass substrates grown at 400 °C. A typical transmission spectrum is shown in Fig. 8. The transmittance in the visible light region is > 85%. The cutoff wavelength extracted from the inflection point is about 380 nm, corresponding to the ZnO bandgap of 3.3 eV. This result indicates that near stoichiometric ZnO films are being grown. For comparison, Fig. 9 shows the room temperature photoluminescence (PL) of ZnO on Corning 7059 glass grown at the same condition. The intense and narrow band edge emission indicates that the ZnO has good crystallinity, while the band edge emission peak at about 380 nm again indicates a ZnO bandgap of ~ 3.3 eV. The doped ZnO films appear to be fairly stable in time as determined from a glass heater test, as shown in Figure 10, wherein the resistance remained constant in time. The photograph in Fig. 11 shows that the ZnO TCO films are adherent to glass, again indicating their usefulness for displays and other applications.

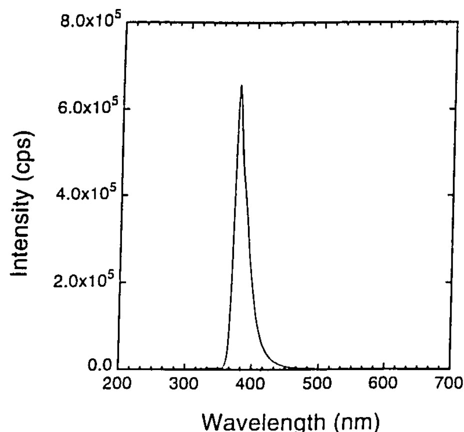

Figure 9. The room temperature PL spectrum of an as-grown ZnO:Ga film on Corning 7079 glass substrate. This film thickness is about 1.2 µm.

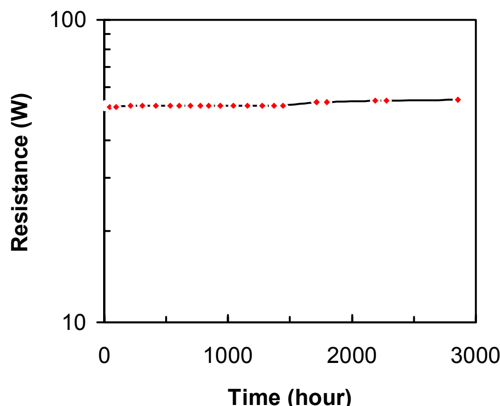

Figure 10. Resistance stability of a transparent ZnO film heating a glass sheet.

An XRD $\theta \rightarrow 2\theta$ scan, using CuKα radiation, was used to determine the crystallinity and preferred orientation of the MOCVD grown films. Shown in Fig. 12 is the XRD $\theta \rightarrow 2\theta$ pattern of a Ga-doped ZnO sample. The substrate is Corning 7059 glass. The growth temperature is 400°C. The film thickness is about 1.2 µm. Similar preferred c-axis oriented ZnO film results were observed from ZnO films deposited on quartz, sapphire, and $LiGaO_2$ substrates except that the Full Wavelength at Half Maxima (FWHM) of the (002) narrowed in going from Corning 7059 glass to sapphire substrates.

In general, we have found ZnO to etch much faster than ITO when using the same acid based etch solutions. However, we have also found that additions of In, Si, Ge and other materials may dramatically change the resistance of the film to chemical attack. By controlling the etchability, conductivity, transmissivity, and so on, we expect that the ZnO alloy material system may find useful applications in a variety of new TCO niches.

Figure 11. Photographic showing of ZnO film adherence using tape test.

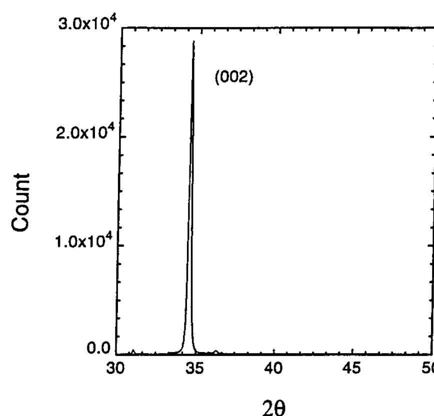

Figure 12. The XRD $\theta \rightarrow 2\theta$ pattern of an as-grown ~1.2 micron thick ZnO:Ga film on Corning 7079 glass substrate. The growth temperature was 400°C. This result reveals a preferred c-axis orientation film.

MOCVD p-TYPE TRANSPARENT AND CONDUCTIVE OXIDE FILM DEVELOPMENT

Table III. Selected listing of ZnO p-type formation efforts.

Summary of p-type deposition runs								Thickness assumed 0.1 micron*				Thickness assumed 0.1 micron*			
								Room Temp (300K)				Low Temp (77K)			
Subst.	Oxidizer	Carrier Gas	N with 10% NH3	Dep, temp, C	4 pt. Sheet Res.	Plasma Fwd/Rev	Thermo Power type	WSU Hall type	WSU (ohm-cm)	WSU (cm^2/V s)	WSU n,p(cm-3)	WSU Hall type	WSU (ohm-cm)	WSU (cm^2/V s)	WSU n,p(cm-3)
glass	O2	Ar		400	1.3E+05	60/8	n	**p**	7.7E+00	0.20	4.0E+18				
glass	O2	N2		400	2.0E+07	70/5	n	n	2.0E+00	1.00	3.0E+18	**p**	6.0E+00	0.06	2.0E+19
SiO2	N2O	N2	Yes	510	4.6E+05	70/10	**p**	n	2.0E+03	0.02	1.0E+16	**p**	2.0E+07	100.00	2.0E+09
SiO2	N2O	N2	Yes	510	4.6E+05	70/10	**p**	n	9.0E+03	0.30	2.0E+14	n	7.0E+06	100.00	1.0E+10
SiO2	N2O	N2	Yes	510	6.9E+05	70/8	**p**	?	>1E07	?	?				
SiO2	O2	N2		375	2.0E+06	none	n	**p**	5.40E+01	0.63	1.8E+17				

*actual thickness not yet calibrated

In the fall of 1997, it was reported in the *Japanese Journal of Applied Physics* by Minegishi et al. of Yamanashi University, that a room temperature p-type, nitrogen doped, transparent conductive zinc oxide (ZnO) film had been formed(39). This followed the 1996 announcement by Tokyo Institute

researchers of p-type CuO alloys[40]. Heretofore, p-type conduction in ZnO had been reported for CVD deposited films at 65 K(41) and < 20 K for N^+ implanted ZnO films(42). Further, a few studies with group I doping elements (Ag, Cu and Li) have shown acceptor-like behavior(43). The II-VI ZnO (3.3 eV) compound is transparent, easily doped n-type to a high conductivity (~10 Ω/), can be made insulating, and is easily produced by MOCVD, as we and others have shown(44,45). Undoped stoichiometric ZnO is highly insulating; however, self-compensating oxygen defects typically generate n-type films and Ga, Al, In, B, and F, among others, are well known to dope ZnO into highly conductive transparent n-type material. Also interesting to note is p-type $SrCu_2O_2$ with which a p-$SrCu_2O_2$/n-ZnO blue/UV LED has been demonstrated(46). To date, we have produced an array of CuAlO, CuAgO and CuGaO, some of which, in preliminary studies, have shown p-type behavior. Further, we have doped ZnO with N to produce p-type films as well, the results of which are shown in Table III.

The significance of a room temperature p-type transparent conductor is vast. First, a transparent p-type conductor now becomes available to increase the efficiency of established emitter and detector applications (such as LEDs, lasers, sensors, and photovoltaics). Second, it allows for development of a new class of transparent devices such as diodes, transistors, detectors, and emitters. It may be possible to make efficient blue/UV oxide LEDs and lasers. ZnO LEDs (or electroluminescent devices) which have primarily been metal semiconductor (MS) devices[47] and occasionally metal-insulator-semiconductor (MIS) devices(48,49,50) up until now have demonstrated extremely low efficiencies. Further, it is even possible that these developments could lead to a new system of solid state oxide lasers; this potentiality is strengthened by the recent demonstration of lasing in ZnO thin films(51,52,53).

Table IV: Example of early evaluation of alternative TCOs for OLEDs. Note the effect of plasma treating the surface.

UPS Results SAMPLE	treatment	Work function (eV)
096 ZnO:Ga	as-received	3.54
096 ZnO:Ga	O2 plasma	4.16
0144 ZnO:Ge	O2 plasma	4.57
0129 GaInO	O2 plasma	3.84
ITO O2 plasma #1	O2 plasma	4.31eV
ITO O2 plasma #2	O2 plasma	4.31eV
0123 ZnInO	O2 plasma	4.46

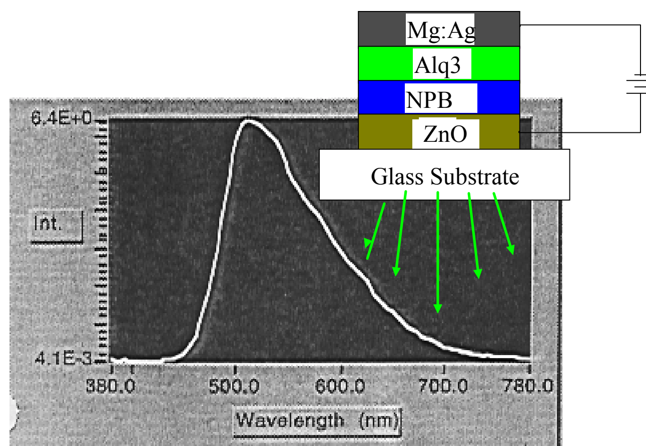

Figure 13. Actual spectral output of an OLED using ZnO:Ga as a replacement to ITO.

One potential area of improvement for Organic Light Emitting Diodes (OLEDs) is in the contact layers—preferably the transparent and conductive layer. Presently, ITO is a well matured technology that is used as the TCO because of its availability and because it works. However, materials with better work functions and bandgap alignment might yield better efficiencies, lifetimes, and so on. Hence, based upon TCO efforts, we have begun evaluating alternative oxide materials. Further, a p-type TCO would be highly advantageous, as shown above, and we are also evaluating these films. Table IV reviews some of our early alternative TCO development efforts. Note the effect of plasma treatment of the surface on the UPS derived work function. These and other results indicate that a superior TCO for OLEDs should be achievable, and should improve device performance. Figure 13 shows the spectral output of a conventional OLED using a ZnO:Ga contact layer in place of ITO.

As an outgrowth of our TCO efforts, we have also evaluated ZnO based thin film materials for their cathodoluminescent and electroluminescent properties[44]. Shown in Figure 15 are the EL spectra and a photograph of one such light emitting film Zn_2SiO_4:Mn. In general, luminescent powders are used

in such applications because of "light piping" effects of solid films diverting photons to the side instead of out to the viewer. We believe the potential of highly luminescent films with design structures merits further investigation.

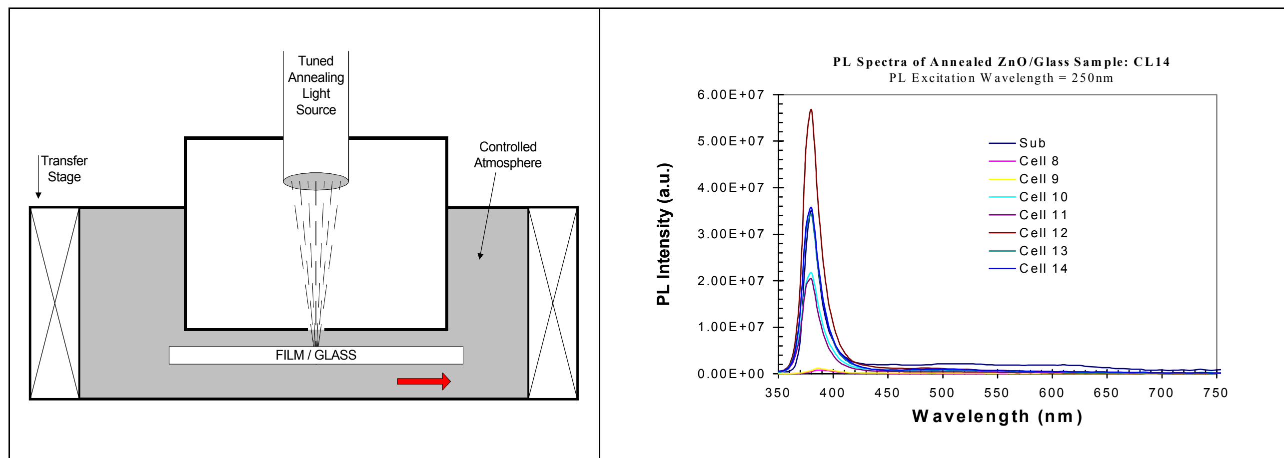

Figure 14. (a) Schematic of laser annealing apparatus, and (b) effects of laser annealing on ZnO photoluminescence. The results show the PL passing through a maximum with increasing annealing time.

An important consideration in film selection is the thermal processing required to obtain useful and optimum properties. In our evaluations of luminescent oxides and TCO films, we are exploring laser annealing of the film in order to process the film at equivalent high effective temperatures without significantly affecting the substrate (typically glass). Figure 14 depicts the effects on ZnO from the as-grown film with increasing laser annealing energy. The effect, under ambient conditions, was for the PL intensity to pass through a maximum before experiencing detrimental effects to the PL. We believe laser annealing may become an extremely useful technology for radically changing oxide film properties, while not modifying surrounding structures.

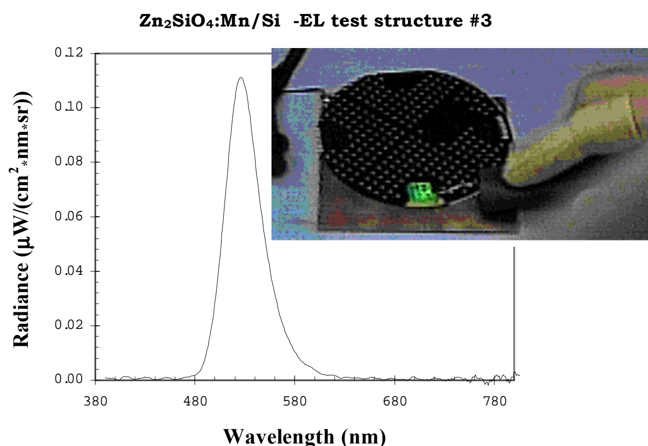

Figure 15. Shown is the EL spectra of a Zn_2SiO_4:Mn sample with the insert showing a photograph of the green light emission.

Figure 16. Cross-sectional SEM photograph of Al_2O_3/ZnO/Si structure of potential use for GaN based materials deposition.

Another derivative application of ZnO may be as an enabling film for producing GaN substrates. GaN is an important wide bandgap material for opto-electronic and high temperature electronic devices.

Unfortunately, high quality large area GaN substrates made from boules are not available. One highly probable substrate approach is to form thick GaN films on top of near-lattice matched substrates, such as $ZnO/LiGaO_2$, or ZnO/Al_2O_3. The important feature is that the thick GaN film can easily be separated from the substrate to thereby produce a GaN substrate—now in the 2”-6” diameter range. Figure 16 shows such a substrate enabling film on a Al_2O_3 substrate.

Lastly, we see many new uses for TCO films in non-TCO applications. One such example is as part of a hydrogen diffusion barrier in a ferroelectric no-volatile memory. ZnO is also well known as a varistor. Another area of rapid development of oxide films is in the area of chemical sensors. Ferroelectrics and GMR oxides are also exciting areas complementing TCO development. Another developing area is oxide optical waveguides with smart switching properties utilizing electroactive elements.

SUMMARY

RDR-MOCVD has been demonstrated for wide range of oxide based (and non-oxide) materials, which have many existing and developing applications. RDR-MOCVD has and is growing oxide films successfully: TCOs, ferroelectrics, dielectrics, phosphors, piezoelectrics, emitters, detectors, and so on. A wide range of precursors and dopants may be utilized, making process development very convenient. Doping of TCO n- and p-type films has been demonstrated; however, much work remains to make routinely useful p-type dopants. RDR-MOCVD can control crystalline, morphological, optical, and electrical properties over wide ranges. SMI is scaling to, mating with, and implementing RDR-MOCVD cluster tool production technology. MOCVD is a dynamic, responsive tool for developing and producing highest quality TCO films.

ABOUT SMI

Structured Materials Industries, Incorporated is focused on being the leader in complex materials Metal Organic Chemical Vapor Deposition (MOCVD) Technology – systems, components, materials, and processes. We have built an in-house multi-reactor base and strategic partnerships to develop and implement oxide MOCVD technology, developed an array of collaborators and customers, and developed a large pool of material and process experience.

ACKNOWLEDGEMENTS

The MOCVD and related projects, whose funding exceeds $4M to date, have been supported by the New Jersey Commission on Science and Technology, the Ballistic Missile Defense Organization (BMDO) with administration by the Air Force, the Army, the Navy and NASA; the NSF; industry; and CRADAs with federal and commercial organizations and laboratories. We acknowledge and are thankful for the benefits of all of these interactions.

REFERENCES

[1] K.L. Chopra, S. Major, and D.K. Pandya, Thin Solid Films 102, 1 (1983).
[2] M. Matsuoka, Jpn. J Appl. Phys. 10, 736 (1971).
[3] S. A. Jerabeck, and S. J. Cardella, Eds., *Transient Voltage Suppression* (General Electric Co., Liverpool, NY, 1986).
[4] M. Watanabe, Jpn. J. Appl. Phys. 9, 418 (1970).
[5] W.S. Lau, J. Vac. Sci. Technol. A 6, 2015 (1988).
[6] Y. Igasaki and H. Saito, J. Appl. Phys. 70, 3612 (1991).
[7] S. Kohiki, M. Nishitani, and T. Wada, J. Appl. Phys. 75 (4), 2069 (1994).
[8] J.B. Webb, D.F. Willams, and M. Buchanan, Appl. Phys. Lett. 39, 640 (1981).

[9] H.K. Kim and M. Mather, Appl. Phys. Lett. 61, 2524 (1992).
[10]H. Sato, T. Minami, Y. Mamura, and S. Takata, Thin Solid Films, 246, 86 (1994).
[11] A. Banerjee, D. Wolf, J. Yang, and S. Guha, J. Appl. Phys. 70, 1692 (1991).
[12] T. Minami, K. Oohashi, and S. Takata, Thin Solid Films 193, 721 (1990).
[13] A. Sarkar, S. Ghosh, S. Chaudhuri, and A.K. Pal, Thin Solid Films 204, 255 (1991).
[14] F. Quaranta, A. Valentini, F.R. Rizzi, and G. Casamassima, J. Appl. Phys. 74, 244 (1993).
[15] D.J. Goyal, C. Agashe, M.G. Takwale, and b.G. Bhide, J. Mater. Res. 8 (5), 1052 (1993).
[16] A. Ghosh and S. Basu, Mater. Chem. Phys. 27, 45 (1991).
[17] M.S. Tomar, Thin Solid Films, 164, 295 (1988).
[18] W. Tang and D.C. Cameron, Thin Solid Films, 238, 83 (1994).
[19] V. Craciun, J. Elders, J.G.E. Gardeniers, and I. W. Boyd, Appl. Phys. Lett. 65 (23), 2963 (1994).
[20]W. Kern and W.C. Heim, J. Electro. Chem. Soc. 117, 562 (1970).
[21] J. Hu and R. G. Gordon, J. Appl. Phys. 71, 880 (1992).
[22] J. Hu and R. G. Gordon, J. Appl. Phys. 72, 5381 (1992).
[23] J. Hu and R. G. Gordon, (a) J. Electrochem. Soc. 139, 2014 (1992), (b) Mater. Res. Soc. Symp. Proc. 242, 743 (1992).
[24] J. Hu and R. G. Gordon, Mater. Res. Soc. Symp. Proc. 283, 891 (1993).
[25] J. Hu and R. G. Gordon, (a) Solar Cells, 30, 437 (1991), (b) Mater. Res. Soc. Symp. Proc. 202, 459 (1991).
[26] C.K. Lau, S.K. Tiku, and K.M. Lakin, J. Electrochem.. Soc. 127, 1843 (1980).
[27] A.P.Roth and D.F. Williams, J. Appl. Phys. 52, 6685 (1981).
[28] J.R. Sheally, B.J. Baliga, R.J. Field, and S.K. Ghandi, J. Electrochem. Soc. 128, 558 (1981).
[29] F.T.J. Smith, Appl. Phys. Lett. 43, 1108 (1983).
[30] W. Kern and W.C. Heim, J. Electro. Chem. Soc. 117, 562 (1970).
[31] K. Tabuchi, W.W. Wenas, A. Yamada, M. Konagai, and K. Takahashi, Jpn. J. Appl. Phys., 32, 3764 (1993).
[32] W.W. Wenas, A. Yamada, M. Konagai, and K. Takahashi, Jpn. J. Appl. Phys., 30, L441 (1991).
[33] H. Sato, T. Minami, S. Takata, T. Miyata, and M. Ishii, Thin Solid Films, 236, 14 (1993).
[34] W. Tang and D.C. Cameron, Thin Solid Films, 238, 83 (1994).
[35] J. Hu and R. G. Gordon, J. Appl. Phys. 71, 880 (1992).
[36] BMDO contracts BMDO/USAS&SDC (Contract No.:DASG60-93-C-0141), BMDO/ONR (Contract No.:N00014-95-C-0234), and BMDO/AF-Rome Laboratories (Contract No.: F19628-96-C-0024).
[37] Y. Li, G.S. Tompa, S. Liang, C.R. Gorla, Y.C. Lu, accepted for publication in JVST, proceedings of the 43rd American Vacuum Society Symposium, 1996.
[38] J. Liu, D.C. Morton, M.R. Miller, Y. Li, and G. S. Tompa, accepted for SID 1997.
[39] K. Minegishi, Y. Koiwai, Y. Kikuchi, K. Yano, M. Kasuga and R. Shimizu, Jpn. J. Appl. Phys., 36, L1453 (1997).
[40] Display Technology News, July 1996, pg. 2.
[41] M. Kasugu and S. Ogawa, Jpn. J. Appl. Phys. 22 (1983) 794.
[42] M. Kasugu and D. Azuma, abstract of 45th Autumn Meeting (1984), Jpn. Soc. Appl. Phys. and Related Soc. 29a-V-s.
[43] Y. Kanik, Jpn. J. Appl. Phys. 30 (1991), pp. 703 and 2021; and A. Valentini, F. Quarante, M. Rossi and G. Battaglia, J. Vac. Sci. & Technol. A9 (1991) 286.
[44] Y. Li, G.S. Tompa, S. Liang, C.R. Gorla, Y.C. Lu, "Transparent and Conductive Ga-Doped ZnO Films Grown by LP-MOCVD" accepted for publciation in JVST, proceedings of the 43rd Amer. Vac. Soc. Symp., 1996; and E.W. Forsythe, Y. Li, D.C. Morton, J. Liu, B.A. Khan and G.S. Tompa, Photoluminescence and Cathodoluminescence of ZnO:Zn Phosphor Films Prepared by MOCVD, Mat. Res. Soc. Symp. Cb14.28, 12/5/96.
[45] For instance, see the many MOCVD works of Prof. Gordon at Harvard.
[46] K. Kawazoe, H. Kawazoe, H. Yanagi, K. Ueda and H. Hosono, MRS Bulletin, August 2000, p. 28-36.
[47] T. Minami, S. Takata, M. Yamanishi, and T. Kawama, Jpn. J. Appl. Phys. 18(18) 1979, p. 1617.
[48] B.W. Thomas and D. Walsh, Electronic Lett. (UK), 9(16) (1973), p. 362.
[49] A. Shimizu, M. Kanbara, M. Hada, and M. Kasuga, Jpn. J. of Appl. Phys., 17 (1978), p. 1435.
[50] T. Minami, M. Tanigawa, M. Yamanishi, and T. Kawamura, Jpn. J. Appl. Phys., 13(9), 1974, p. 1475.
[51] I. Akasaki, and H. Amano, Materials Research Society Fall Meeting, Boston, MA, 1991.
[52] S. Nakamura, M. Senoh, and T. Mukai, Jpn. J. Appl. Phys. **30**, L1708, 1991; S. Nakamura, T. Mukai, and M. Senoh., Jpn. J. Appl. Phys. **30**, L1998, 1991.
[53] D. C. Reynolds, D. C. Look, and B. Jogai, Solid state Communication, **99**, No. 12, pp. 873-875, 1996.